# Deoxyinosine mismatch parameters calculated with a mesoscopic model result in uniform hydrogen bonding and strongly variable stacking interactions

Rodolfo Vieira Maximiano[a,b], Gerald Weber[a]

[a]*Departamento de Física, Universidade Federal de Minas Gerais, 31270-901, Belo Horizonte-MG, Brazil*
[b]*Centro Federal de Educação Tecnológica de Minas Gerais, 32210-160, Contagem-MG, Brazil*

## Abstract

Here we apply a technique which uses mesoscopic models to calculate hydrogen bond strengths and stacking interactions from experimental deoxyinosine melting temperatures. Our results confirm a uniform hydrogen bond strength for all deoxyinosine mismatches of the same order of AT base pairs, with the only exception of II mismatches which show a reduced hydrogen bonding. The resulting stacking interactions however are far from uniform, with IG showing the largest variations. The highly asymmetric stacking directly influences the duplex stability and calculated opening profiles show that for some mismatches there can be localized break down of the melting cooperativity.

*Keywords:* Deoxyinosine, Peyrard-Bishop DNA models, DNA stability, DNA mesoscopic models, hydrogen bonds, stacking interactions

## 1. Introduction

Inosine occurs naturally in tRNA where it pairs equally to cytosine, adenine and uracil. When used in DNA it has found practical applications as a "universal" base. For instance, in 1985 the use

---

*Corresponding author
Email address:* gweberbh@gmail.com (Gerald Weber)

of inosine was already extensively discussed for probe design [1, 2, 3], and applications of inosine for PCR primer design were reported [4, 5]. More recent examples are its use in sequencing by ligation, a next-generation sequencing technique where the use of inosine is thought to increase the read lengths [6, 7] and for directional cloning [8].

Early thermodynamic studies of deoxyinosine were performed by Kawase *et al.* [9], and Case-Green and Southern [10]. However, most of our current knowledge of the basic properties of deoxyinosine come from comprehensive UV measurements by Watkins *et al.* [11]. From nearest-neighbour free energy models they derived a generalized stability trend IC > IA > IT ≈ IG > II which is widely used in practical applications [12, 8]. Further detailed properties of hydrogen bonds were obtained from NMR [13, 14, 15] and x-ray measurements [16, 17]. All these studies suggest a configuration of two hydrogen bonds for all inosine mismatches.

From a theoretical point of view only hypoxantine, the nucleobase of inosine, was studied with density functional theory (DFT) [18, 19, 20]. However, these results are difficult to correlate with inosine, especially for the lack of the phosphate backbone in those calculations [18, 19, 20]. Molecular dynamics were performed by Krepl *et al.* [21] for one DNA sequence containing inosine IC mismatch who concluded that the reduced stability is not solely due to the reduced number of hydrogen bonds when compared to guanine.

The thermodynamic analysis of oligonucleotides by mesoscopic models employing experimental melting temperatures is emerging as a way to independently study the hydrogen bond and stacking interactions [22, 23]. Given the practical interest of inosine it is worthwhile to extend the investigation of its thermal properties with mesoscopic models.

The basis of our mesoscopic model is the Peyrard-Bishop (PB) model [24]. This is a statistical mechanics model where the main features are based on Morse potentials for the hydrogen bonds interaction and stacking interactions between adjacent base pairs along the DNA strand. This model has the advantage to allow us to obtain the hydrogen bonds and stacking interaction strengths from melting temperatures, as we showed for DNA [22] and RNA [23]. Therefore, the PB model overcomes some of the limitations attributed to free-energy models [21, 25, 26]. Recent results [27] indicate there is a also a possibility of obtaining structural parameters such as the helicoidal rise step of DNA.

2

The PB model is under active development and routinely applied to a number of different physical situations involving oligonucleotides. Some recent examples are its use to study mecanical unzipping [28], charge transport in DNA [29, 30], the multifractal properties of DNA denaturation [31], DNA over-stretching transition [32], the behaviour of DNA in external fields [33], and thermal switching in DNA devices [34]. Another interesting example of application is its use in the study of promoters in cyanobacteria [35] and promoter clustering [36]. One interesting property of the model is that it is easily adaptable to describe further interactions such as the influence of solvent [37, 38, 39], it is also being used for in depth studies of mathematical properties of these type of system [40]. Another mesoscopic model of interest is the rodlike polyelectrolyte model which was recently used for the description of salt-dependent DNA melting [41]

Here we analyse the melting temperatures of sequences containing inosine mismatches from Ref. 11 with the Peyrard-Bishop (PB) model. We were able to obtain a complete description of inosine hydrogen bonds and related stacking parameters. The calculated Morse potentials are consistent with a chemical structure formed by two hydrogen bonds, of similar strength as for AT, for all inosine mismatches. In contrast, the calculated stacking interactions were found to be very dissimilar to that of canonical DNA, with the exception of IC mismatches. Further calculations of helix opening profiles show that the strong variations in stacking interaction result in some large opening amplitudes. In the case of IG and IA mismatches, this disturbance can be strong enough to promote a localized break down of the melting cooperativity.

## 2. Materials and Methods

### 2.1. Melting temperature dataset

The sequences used for the calculations in this work are UV absorption measurements from Watkins *et al.* [11], composed of 84 sequences in addition to 13 sequences from other sources [2, 42]. These sequences were designed in such a way as to cover every possible neighbouring interaction for a given inosine mismatch pair. The experimental error reported for the melting temperature estimations is 0.3 °C for the 84 oligonucleotide duplexes, which have lengths of either 9 or 12 base pairs (bp) [11]. All sequences are shown in supplementary Tables S1–S5. They are presented with

their experimental melting temperature, the calculated melting index, and the predicted melting temperature obtained using the newly calculated parameters. For the minimization the dataset was divided into groups of sequences that contained a particular IX mismatched pair, where X=A, C, G, T or I. This results in smaller datasets specific to each inosine mismatch (one for IA, another for IC, etc). Tandem inosine mismatches were not included in this analysis as they were too few of them for applying the parameter fitting method [22]. Also, the sequences described as NN outliers of Ref. 11 decreased the quality of the results as melting temperature prediction became poorer for all sequences (data not shown), and therefore these sequences were not included in our dataset.

## 2.2. The Peyrard-Bishop model

We use a PB model [24] with simple harmonic stacking interactions. The main components of the PB model are the hydrogen bond between the bases of a pair, represented by a Morse potential, and the stacking interaction between nearest neighbours, represented by a harmonic potential in this case. For the example of an IA base pair, the corresponding representation of these terms are

$$V(y_{IA}) = D_{IA}\left(e^{-y_{IA}/\lambda_{IA}} - 1\right)^2 \tag{1}$$

which corresponds to a Morse potential between inosine (I) on one strand with the opposing adenine (A) on the other strand, and $y$ represents the relative distance between the bases. The Morse parameter $D$ largely accounts for the hydrogen bond strength, while $\lambda$ represents the potential width.

Expanding the previous example for an IA base pair adjacent to CG (IApCG), the stacking interaction is given by

$$w(y_{IA}, y_{CG}) = \frac{k_{IApCG}}{2}(y_{IA}^2 - 2y_{IA}y_{CG}\cos\theta + y_{CG}^2) \tag{2}$$

The elastic constant $k$ represents the interaction between stacked bases, and $\theta$ is a small angle (0.01 rad) introduced to prevent numerical divergence in the integration procedure [43].

The average distance for the $m$-th base pair can then be calculated from

$$\langle y_m \rangle = \frac{1}{Z_y} \int \prod_n y_m e^{-\beta[w(y_n, y_{n-1}) + V(y_n)]} dy_n \tag{3}$$

4

where $Z_y$ is the classical partition function for this Hamiltonian [45]. Both the partition function $Z_y$ as well as the distance $\langle y_m \rangle$ are calculated numerically with the transfer integral technique [43].

Eqs. (1) and (2) are the potentials used for the calculation of the classical partition function from which we calculate a melting index $\tau$ for each sequence [44]. The melting index is calculated from a numerical expansion of the partition function $Z_y$ in terms of the non-diagonal components of the transfer integral matrix. The basis functions of the expansion are taken from a homogeneous sequence composed of CG base pairs only, see Fig. 2 of Ref. 44. In practice, the melting index represents how much a given sequence difers from a CG-only sequence by taking into account the interaction potentials. The resulting melting indexes are then correlated to the experimental melting temperatures using linear regression. Further details concerning the model implementation are described in Refs. 44 and 45, and a free software implementation is reported in Ref. 46.

## 2.3. Optimization of the model parameters

To optimize the PB model parameters we let them evolve from a predetermined starting point until we arrive at values that are able to minimize the square differences between experimental melting temperature $T_i$, and predicted melting temperature $T_i'$ of a particular sequence $i$, for all $N$ sequences of the dataset. This is represented as minimizing $\chi^2$

$$\chi^2 = \sum_{i=1}^{N} (T_i' - T_i)^2 . \tag{4}$$

We will also refer to the average melting temperature deviation $\Delta T$

$$\langle \Delta T \rangle = \frac{1}{N} \sum_{i=1}^{N} \left| T_i' - T_i \right| . \tag{5}$$

The predicted melting temperature $T_i'$ of a given sequence can be calculated from its melting index $\tau_i$ which is given by the PB model [44].

Unlike our previous calculations with DNA [22] and RNA [23], we could not implement a length dependence regression due to insufficient variability of sequence lengths (mostly 12 pb) in the dataset or Ref. 11. Therefore, we employed a single linear regression equation, without length dependence,

$$T_i' = f_0 + f_1 \tau_i, \tag{6}$$

5

where $f_0$ and $f_1$ are linear regression coefficients calculated for all sequences that belong to a particular mismatch, for instance I.A.

### 2.3.1. Minimization procedure

The single-equation regression scheme, Eq. (6), generally presents poorer results than the two-equation regression [23] since the best global minima of $\chi^2$ is much more difficult to find. Therefore the minimization procedure was adapted in the following way:

**Initial minimization**  All stacking and Morse potentials are allowed to vary simultaneously. For each minimization round the initial parameters change randomly within the interval of 16.5 meV and 49.5 meV. This interval corresponds to a variation of ±50% of the Morse parameter of the AT base pair ($D_{AT}$ = 33 meV). Similarly, all initial stacking parameters are values chosen in the range between 1.25 eV/nm$^2$ and 3.75 eV/nm$^2$. We repeated this procedure 1000 times, which takes around 600 hours of processing time on 1.6 GHz processors. The resulting value of each parameter is obtained by averaging over all results provided by the minimization.

**Final minimization**  We use the averaged results from the previous round as new initial parameters. But this time, instead of varying the initial parameters, the experimental dataset is randomly changed by small amounts according to the declared experimental error in the temperature measurements, 0.3 °C in this case [11]. In this way we can estimate the experimental error influence on our parameters [22]. As in the initial minimization, all parameters are allowed to vary during minimization with the goal of obtaining the smallest $\chi^2$. This procedure was repeated again 1000 times. At the end we obtained both the standard deviation and the final optimum value for each parameter.

### 2.4. Availability

The inosine parameters calculated in this work were included in version 2.0 of our TfReg software[46], and can be found at `https://sites.google.com/site/geraldweberufmg/tfreg`.

## 3. Results and Discussion

### 3.1. Parameter optimization

The present analysis differs from our previous calculations for DNA and RNA [22, 23] in two essential ways. One is that it is an application of the Peyrard-Bishop model to non-canonical nucleotides and base-pairs that are mismatched, which to our knowledge has not been attempted before. The second is that the available inosine dataset contains no diversity of sequence lengths, which makes it impossible to apply the length dependent melting temperature regression developed for DNA [44]. Instead we have to recur to a single equation for the regression, Eq. (6), which was first introduced for an initial analysis of RNA [23]. This has resulted in a difficult convergence of $\chi^2$ values during initial step of the minimization procedure, which is the reason why a rather large number of minimization steps was necessary. Fortunately, these limitations did not prevent us from obtaining fairly consistent results. After performing the two minimization rounds, described in Materials and Methods, we obtained an average temperature deviation $\langle \Delta T \rangle$ of 1.1 °C using the melting index technique [44]. Note that this is practically identical to the temperature deviation of 1.2 °C obtained from nearest-neighbour calculations reported by Watkins *et al.* [11].

While the quality of prediction of the PB model and the nearest-neighbour calculations are comparable, the PB model offers a more intuitive interpretation of the model parameters. This is nicely illustrated in Table 1 where we present the resulting Morse potential parameters which are related to hydrogen bond strengths. The four inosine mismatches which pair with canonical nucleotides (A, C, G and T) resulted in Morse parameters similar to the Watson-Crick base pair AT of 33 meV [22]. This is consistent with the established view that two hydrogen bonds are formed for these inosine mismatches [11, 2, 15]. The potential $\lambda$ for IA, IC and IG are mostly within the range of AT ($3.2 \times 10^{-2}$ nm). However, for IT and II we observe an important increase, Tab. 1, indicating a small widening of the potential.

The similarity of all four hydrogen bonds of inosine-canonical mismatches would support the suggested role of inosine as a universal base. However, the calculated stacking parameters clearly dispel this notion. A large part of these parameters fall outside the DNA range of 1 eV/nm$^2$ to 4 eV/nm$^2$ [22], as shown in Table 2. Only IC is reasonably contained within the canonical

Table 1: Inosine Morse potential parameters. The Morse potentials $D$ are given in meV and $\lambda$ in $10^{-2}$ nm. In parenthesis are the standard deviations, obtained from the final minimization round, in compact uncertainty notation.

|  | IA | IC | IG | IT | II |
|---|---|---|---|---|---|
| $D$ | 31(4) | 34(2) | 38(2) | 29(5) | 24(5) |
| $\lambda$ | 2.9(9) | 3.2(2) | 3.0(3) | 4.9(2) | 3.8(1) |

DNA range. At the extreme ends of the stacking parameter range is IG with the largest difference, 0.013–12.5 eV/nm$^2$, and IA with the second largest difference 0.0002–7.0 eV/nm$^2$. One explanation for the extreme stacking parameters of IG could be that it is the only mismatch in syn-anti configuration [11]. Rutledge *et al.* [19], who performed a density functional theory (DFT) analysis on hypoxanthine also reported considerable buckle and propeller distortions for guanine mismatches. On the other hand, IC is reasonably contained within Watson-Crick base pair range possibly because inosine is closest to guanine. In other words, IC stacking resembles more closely a Watson-Crick GC base pair than any other inosine mismatch, which is consistent with the similarity between inosine and guanine.

Nearest-neighbour (NN) parameters of free-energy (FE) models also present very large variations as the PB stacking parameters, in certain cases up to an order of magnitude [11]. For instance, for IA mismatches the FE parameter $\Delta G^{\circ}_{37}$ are 0.09 kcal/mol and −1.24 kcal/mol, for AIpAT and AIpCG nearest-neighbours, respectively. Another example is for the case of II mismatches $\Delta G^{\circ}_{37}$ of -0.09 kcal/mol and 0.81 kcal/mol for GCpII and IIpAT, respectively. However, correlating linear FE parameters to PB parameters is usually not meaningful [47] since PB parameters are non-linear and the model considers NN and base-pair interactions separately. Instead, we will discuss the overall stability of the inosine mismatches in terms of the average openings $\langle y \rangle$, Eq. (3), calculated with the new parameters. The average openings provide a view on sequence stability which differs from Gibbs free energy estimates. The value of $\Delta G$ indicates the likelihood that a given structure may hybridize spontaneously at a given temperature. In contrast, average openings $\langle y \rangle$ provide a more detailed view of helix denaturation by calculating the distance of

Table 2: Stacking parameters $k$ in eV/nm$^2$. In parenthesis are the standard deviations in compact uncertainty notation. The table is divided into three parts, with the central section representing stacking parameters in the same range as for Watson-Crick base pairs [22].

| Range | IA | | IC | | I.G | | IT | | I.I | |
|---|---|---|---|---|---|---|---|---|---|---|
| | ATpAI | 0.0002* | | | ATpGI | 0.013(5) | ATpIT | 0.24(8) | IIpAT | 0.09(3) |
| | AIpAT | 0.20(6) | | | IGpAT | 0.043(9) | ATpTI | 0.6(2) | ATpII | 0.8(2) |
| | IApAT | 0.9(2) | | | GIpAT | 0.12(2) | ITpAT | 0.9(2) | | |
| < 1 | | | | | CGpIG | 0.69(7) | | | | |
| ≥ 1 | | | CGpCI | 1.30(9) | | | TApIT | 1.5(3) | | |
| | | | CIpAT | 1.8(1) | | | | | | |
| | | | CIpCG | 1.57(1) | | | | | | |
| ≥ 2 | AIpTA | 2.2(3) | ATpCI | 2.2(1) | CGpGI | 2.0(2) | GCpIT | 2.7(4) | CGpII | 2.6(4) |
| | AIpGC | 2.2(3) | ATpIC | 2.6(2) | | | CGpTI | 2.8(4) | | |
| | | | ICpAT | 2.9(2) | | | | | | |
| ≥ 3 | CGpAI | 3.4(3) | GCpCI | 3.4(2) | | | | | | |
| < 4 | | | CGpIC | 3.8(2) | | | | | | |
| ≥ 4 | AIpCG | 5.1(4) | | | GCpIG | 4.6(3) | CGpIT | 5.9(4) | GCpII | 4.6(6) |
| | GCpAI | 7.0(5) | | | ATpIG | 5.8(4) | GCpTI | 6.9(4) | | |
| | | | | | GCpGI | 12.5(4) | | | | |

*the standard deviation for this parameter is 0.004 eV/nm$^2$

base pairs along the sequence.

Fig. 1 shows the calculated opening profiles $\langle y \rangle$ as a function of temperature for some inosine mismatches embedded in a CAAAIAAAG sequence. This sequence was used by Martin *et al.* [2] which is one of the earliest studies on inosine. A smaller average opening $\langle y \rangle$ at a given base pair means that the sequence is locally more stable at a given temperature. IC mismatches present an almost identical opening profile to AT base pairs, while IG in contrast destabilizes the duplex quite strongly. Furthermore, the IG mismatch causes a much increased base pair amplitude on the right-hand side of the duplex, where there is a much weaker stacking interaction. This asymmetric disturbance propagates along all sites towards the right-hand side terminal, and remains even at
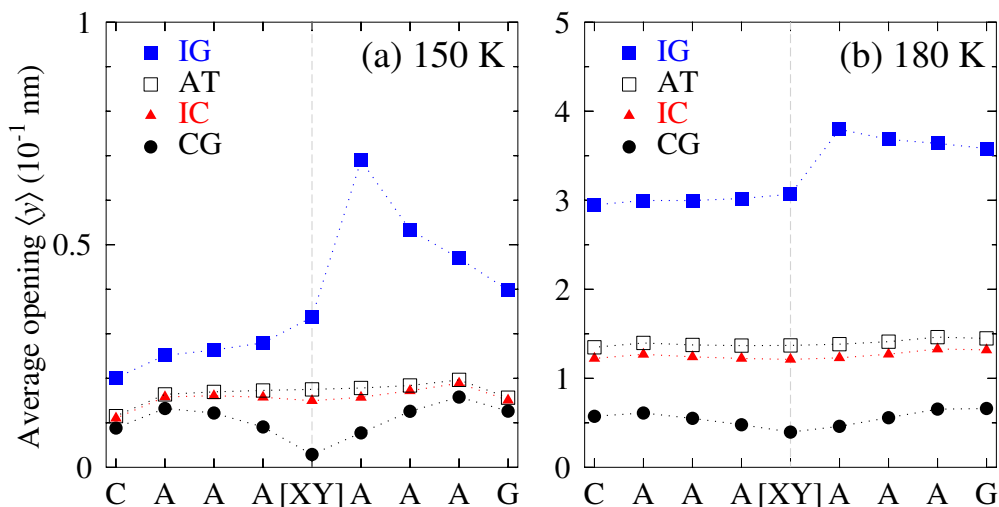
Figure 1: Average opening profiles $\langle y \rangle$ as a function of base pair position of sequences of type CAAA[XY]AAAG, where XY is either IG (blue boxes), AT (squares), IC (red triangles) or CG (bullets). The position of the XY base pair is shown as a light grey vertical dashed line. Profiles were calculated at (a) 150 K and (b) 180 K. Please note that these temperatures are unrelated to the predicted melting temperature as discussed in Ref. 22.

higher temperatures

IA mismatches also have similar variable stacking interactions as IG, shown in Tab. 2. In Fig. 2 we show an example where an IA mismatch is placed at the 5th position of a 14 bp long sequence. Even at low temperatures the IA mismatch strongly disturbs the duplex with very large but localized average openings. Interestingly, at a somewhat larger temperature the average helix opening is much larger on the left-hand side despite being composed of strongly bonded CG base pairs. Adding further CG base pairs at the left-hand side dampens these amplitudes as shown in Fig. 3a. Yet as we increase the temperature to 240 K, Fig. 3b, even these additional CG base pairs have little effect in dampening the motion amplitude. An intriguing aspect that emerges from Fig. 3 is that the strong discontinuity of the stacking parameters essentially isolates each side of the sequences. The right-hand side is completely undisturbed by the additional CG base pairs on the left-hand side. Therefore, what we are observing appears to be a breakdown of the base pair cooperativity within the DNA sequence induced by the IA mismatch [48].

The cooperativity breakdown shown in Figs. 2 and 3 suggest uses of technological interest for inosine mismatches beyond that of probe design. For instance, the difference in motion am-
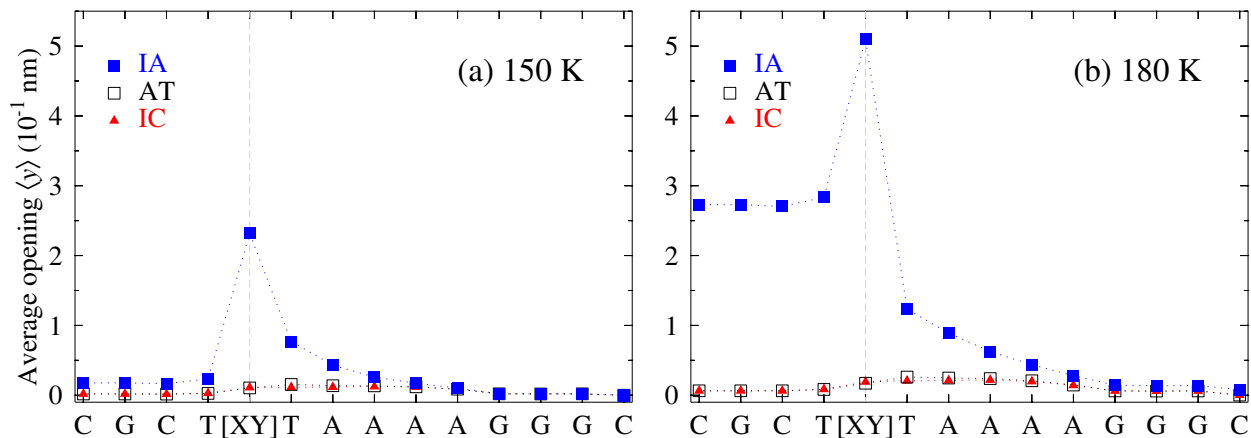
10

Figure 2: Average opening profiles $\langle y \rangle$ as function of base pair position of sequences of type CGCT[XY]TAAAAGGGC, where XY is either IA (blue boxes), AT (squares) or IC (red triangles). The position of the XY base pair is shown as a light grey vertical dashed line. Profiles were calculated at (a) 150 K and (b) 180 K.
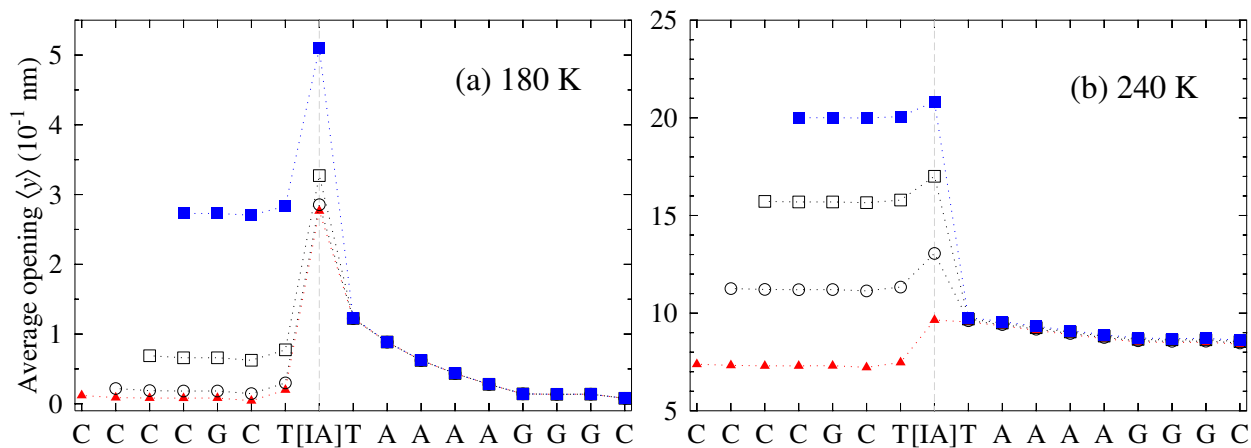


Figure 3: Average opening profiles $\langle y \rangle$ as function of base pair position of sequences of increasing length with IA mismatch (light grey vertical dashed line) calculated at (a) 180 K and (b) 240 K. The first sequence is the same as of Fig. 2 and shown as blue boxes. The three remaining sequences are as the first with one (squares), two (circles) or three (red triangles) additional CG base pairs at the left-hand side.

plitude on each side of a sequence containing IG or IA mismatches should affect applications which depend on FRET, which is highly sensitive to donor-acceptor distances [49]. But perhaps more interestingly could be its use as thermal rectifier, a role that was suggested for normal DNA sequences [34, 50].

## 4. Conclusions

In this work we have obtained the Peyrard-Bishop parameters, both for Morse potential and elastic constants for sequences containing inosine mismatches in DNA. Such parameters were calculated from published melting thermodynamics datasets and were used to predict melting temperatures and general stability trends for inosine mismatches. The calculated parameters which represent hydrogen bonding are in agreement with the notion of all inosine mismatches being formed by two hydrogen bonds. The stacking parameters are distributed over a much wider range than for canonical DNA base pairs. In some cases, such as IA and IG mismatches, these stacking parameters take either very low or very high values which causes a disruption in the melting cooperativity along the chain of DNA base pairs.

**Supplementary information**

Tables S1–S5 show the sequences used and predicted melting temperatures obtained with the inosine parameters.

**References**

[1] Y. Takahashi, K. Kato, Y. Hayashizaki, T. Wakabayashi, E. Ohtsuka, S. Matsuki, M. Ikehara, K. Matsubara, Proceedings of the National Academy of Sciences 82 (7) (1985) 1931–1935.

[2] F. H. Martin, M. M. Castro, F. Aboul-ela, I. Tinoco, Nucleic Acids Research 13 (24) (1985) 8927–8938.

[3] E. Ohtsuka, S. Matsuki, M. Ikehara, Y. Takahashi, K. Matsubara, J. Biol. Chem. 260 (5) (1985) 2605–2608. arXiv:http://www.jbc.org/cgi/reprint/260/5/2605.pdf.
URL http://www.jbc.org/cgi/content/abstract/260/5/2605

[4] G. M. Rossolini, S. Cresti, A. Ingianni, P. Cattani, M. L. Riccio, G. Satta, Molecular and Cellular Probes 8 (2) (1994) 91–98.

[5] D. Loakes, Nucl. Acids. Res. 29 (12) (2001) 2437–2447.

[6] A. Ho, M. Murphy, S. Wilson, S. R. Atlas, J. S. Edwards, BMC Genomics 12 (1) (2011) 598.

[7] Z. Yu, Engineering 5 (2013) 440.

[8] T. Baumann, K. M. Arndt, K. M. Müller, BMC Biotechnology 13 (1) (2013) 81.

[9] Y. Kawase, S. Iwai, H. Inoue, K. Miura, E. Ohtsuka, Nucleic Acids Research 14 (19) (1986) 7727–7736.

[10] S. C. Case-Green, E. M. Southern, Nucl. Acids. Res. 22 (2) (1993) 131–136.

[11] J. Watkins, Norman E., J. SantaLucia, John, Nucl. Acids. Res. 33 (19) (2005) 6258–6267. arXiv:http://nar.oxfordjournals.org/cgi/reprint/33/19/6258.pdf, doi:10.1093/nar/gki918.
URL http://nar.oxfordjournals.org/cgi/content/abstract/33/19/6258

[12] C. Öhrmalm, M. Jobs, R. Eriksson, S. Golbob, A. Elfaitouri, F. Benachenhou, M. Strømme, J. Blomberg, Nucleic Acids Research 38 (21) (2010) e195. doi:10.1093/nar/gkq777.

[13] S. Uesugi, Y. Oda, M. Ikehara, Y. Kawase, E. Ohtsuka, J. Phys. C: 262 (15) (1987) 6965–6968. arXiv:http://www.jbc.org/cgi/reprint/262/15/6965.pdf.
URL http://www.jbc.org/cgi/content/abstract/262/15/6965

[14] Y. Oda, S. Uesugi, M. Ikehara, Y. Kawase, E. Ohtsuka, Nucleic Acids Research 19 (19) (1991) 5263–5267.

[15] E. M. Basílio Janke, F. Riechert-Krause, K. Weisz, The Journal of Physical Chemistry B 115 (26) (2011) 8569–8574.

[16] P. W. R. Corfield, W. N. Hunter, T. Brown, P. Robinson, O. Kennard, Nucleic Acids Research 15 (19) (1987) 7935–7949.

[17] W. B. T. Cruse, J. Aymani, O. Kennard, T. Brown, A. G. C. Jack, G. A. Leonard, Nucleic Acids Research 17 (1) (1989) 55–72.

[18] G. Paragi, I. Pálinkó, C. Van Alsenoy, I. K. Gyémánt, B. Penke, Z. Timár, New Journal of Chemistry 26 (10) (2002) 1503–1506.

[19] L. R. Rutledge, C. A. Wheaton, S. D. Wetmore, Physical Chemistry Chemical Physics 9 (4) (2007) 497–509.

[20] L. R. Rutledge, S. D. Wetmore, Physical Chemistry Chemical Physics 14 (8) (2012) 2743–2753.

[21] M. Krepl, M. Otyepka, P. Banáš, J. Šponer, The Journal of Physical Chemistry B 117 (6) (2013) 1872–1879.

[22] G. Weber, J. W. Essex, C. Neylon, Nature Physics 5 (2009) 769–773. doi:10.1038/nphys1371.

[23] G. Weber, Nucl. Acids. Res. 41 (2013) e30. doi:10.1093/nar/gks964.
URL http://nar.oxfordjournals.org/content/early/2012/10/18/nar.gks964.short

[24] M. Peyrard, A. R. Bishop, Phys. Rev. Lett. 62 (23) (1989) 2755–2757.

[25] J. Šponer, C. A. Morgado, D. Svozil, The Journal of Physical Chemistry B 116 (28) (2012) 8331–8332.

[26] C. A. Johnson, R. J. Bloomingdale, V. E. Ponnusamy, C. A. Tillinghast, B. M. Znosko, M. Lewis, The Journal of Physical Chemistry B 115 (29) (2011) 9244–9251.

[27] T. D. Amarante, G. Weber, Journal of Physics: Conference Series 490 (1) (2014) 012203.

[28] S. Buyukdagli, M. Joyeux, Chemical Physics Letters 484 (4) (2010) 315–320.

[29] A. Shigaev, O. Ponomarev, V. Lakhno, Chemical Physics Letters 513 (4) (2011) 276–279.

[30] G. Kalosakas, Phys. Rev. E 84 (2011) 051905. doi:10.1103/PhysRevE.84.051905.
URL http://link.aps.org/doi/10.1103/PhysRevE.84.051905

[31] S. Behnia, A. Akhshani, M. Panahi, A. Mobaraki, M. Ghaderian, Phys. Lett. A 376 (2012) 2538–2547.

[32] A. E. B. Pupo, F. Falo, A. Fiasconaro, The Journal of Chemical Physics 139 (9) (2013) 095101.

[33] A. Bergues-Pupo, J. Bergues, F. Falo, Physica A: Statistical Mechanics and its Applications 396 (2014) 99–107.

[34] C.-C. Chien, K. A. Velizhanin, Y. Dubi, M. Zwolak, Nanotechnology 24 (9) (2013) 095704.

[35] H.-H. Huang, P. Lindblad, J. Biol. Eng 7 (10).

[36] L. Pettinato, E. Calistri, F. Di Patti, R. Livi, S. Luccioli, PloS One 9 (1) (2014) e85260.

[37] G. Weber, Europhys. Lett. 73 (5) (2006) 806–811. doi:10.1209/epl/i2005-10466-6.

[38] D. X. Macedo, I. Guedes, E. L. Albuquerque, Physica A: Statistical Mechanics and its Applications.

[39] A. Singh, N. Singh, Physica A: Statistical Mechanics and its Applications 392 (9) (2013) 2052–2059.

[40] R. F. Álvarez-Estrada, G. F. Calvo, H. Serrano, Journal of Computational and Applied Mathematics 236 (15) (2012) 3561–3571.

[41] C. B. Passos, P. S. Kuhn, M. C. Barbosa, Physica A: Statistical Mechanics and its Applications 413 (2014) 481–488.

[42] D. E. Bergstrom, P. Zhang, W. T. Johnson, Nucleic Acids Research 25 (10) (1997) 1935–1942.

[43] Y.-L. Zhang, W.-M. Zheng, J.-X. Liu, Y. Z. Chen, Phys. Rev. E 56 (6) (1997) 7100–7115.

[44] G. Weber, N. Haslam, N. Whiteford, A. Prügel-Bennett, J. W. Essex, C. Neylon, Nature Physics 2 (2006) 55–59. doi:10.1038/nphys189.

[45] G. Weber, N. Haslam, J. W. Essex, C. Neylon, J. Phys. Condens. Matter 21 (2009) 034106. doi:10.1088/0953-8984/21/3/034106.

[46] G. Weber, Bioinformatics 29 (2013) 1345–1347. doi:10.1093/bioinformatics/btt133.
URL http://bioinformatics.oxfordjournals.org/content/early/2013/03/16/bioinformatics.btt133.abstr

[47] G. Weber, Europhys. Lett. 96 (2011) 68001.
URL http://iopscience.iop.org/0295-5075/96/6/68001

[48] S. Ares, N. K. Voulgarakis, K. Ø. Rasmussen, A. R. Bishop, Phys. Rev. Lett. 94 (2005) 035504.

[49] S. Khrapunov, M. Brenowitz, Biophysical journal 86 (1) (2004) 371–383.

[50] M. Terraneo, M. Peyrard, G. Casati, Phys. Rev. Lett. 88 (9) (2002) 094302.